

FIRST SIMULATION RESULTS ON FREE ELECTRON LASER RADIATION IN DISPLACED PHASE-COMBINED UNDULATORS*

N.S. Mirian,[†]

UVSOR Facility, Institute for Molecular Science (IMS), Okazaki, Japan and
School of Particle and Accelerator Physics, IPM, Tehran, Iran

E. Salehi, Department of Physics, Amirkabir University of Technology, Tehran, Iran

Abstract

This report deals with self amplified spontaneous emission free electron laser (FEL) amplifier where the FEL emission is obtained from displaced phase combined undulators. Magnetic field of this adjustment methods in three dimensions is presented. The electron dynamics is investigated. The simulation method and results are explained. The radiation properties of the fundamental resonance and third harmonic through the phase combined undulators are compared with the normal undulator with the same undulator deflection parameter.

INTRODUCTION

In free electron laser (FEL), a relativistic and high current electron beam passes through a periodic, transverse magnetic undulator field and produces electromagnetic wave. Undulator, as a major component in the FEL, converts the energy of the electron beam to that of the radiation field [1,2].

We know that when the gap between the top and bottom magnetic arrays is relatively narrow, the magnetic arrays of undulators subject to a significant attractive force. Therefore, the undulators usually require rigid mechanical components and frames to control the magnetic gap precisely. Further, a large number of components are required to administrate the mechanical load along the undulator axis and forbear the deformation of the magnetic arrays. If we remove the attractive force between the two arrays of the undulator, the heavy and large base frame is not necessary, and the undulator will be designed to be much more compact and lightweight.

Recently, Kinjo et. al in Ref. [3] have employed phase-combined undulators (PCUs) in two new methods to make fine adjustment of the magnetic force in the insertion device. In the PCUs the phase between the lower and upper Halbach arrays is shifted such that the undulator has no magnetic force without using any cancellation system. By developing the principle of PCU, Kinjo et al. [3] divided the undulator into a number of sections such that half of them are phase-shifted in one direction and the others are shifted in opposed direction, without breaking the periodic condition in the undulator field. In their first method, they suggested an additional phase shift by a relative longitudinal displacement of δ to each section of the PCU; this method is referred to as the displacement method. In the second method, they used the

easy axis rotation, which is hereinafter referred to as the rotation method.

In this report, we investigate the evolution of the electron beam and radiation in the FEL by employing the displaced PCU.

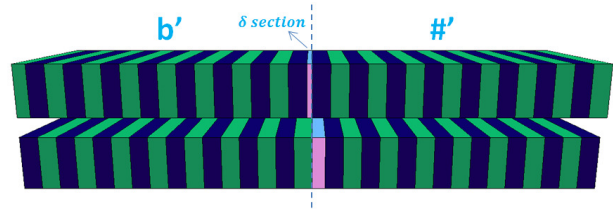


Figure 1: Conceptual diagram of the PCU.

GENERAL DISCUSSION

According to Ref. [3], by displacing upper or lower magnet array by $-\lambda_u/4$, the vertical force between the two arrays can be eliminated; while the shear longitudinal force that appears in the two arrays may be positive or negative depending on whether the upper or lower magnetic array is displaced. For significant reduction of the attractive force between the two arrays and longitudinal force, the PCU is composed of two kinds of sections as shown in Fig. 1. The blue blocks show the vertical polarization and the green blocks show the horizontal polarization. In one kind of section called b' , the upper magnets array are displaced by $-\lambda_u/4$, while in the next kind of section called $\#$, the lower magnets array are displaced by $-\lambda_u/4$. Composition of these two sections can eliminate the shear longitudinal force. In the displacement adjusting method the relative longitudinal displacement of δ is added to each section, as shown in Fig. 1. In this figure, D shows the number of sections and the symbol $\#'$ (b') denotes the lower (upper) array of magnets that is displaced by $-\lambda_u/4 - \delta$. Then, the magnetic field in three dimensions takes form

$$\mathbf{B}_{\#', b'} = \begin{bmatrix} \pm \frac{B_0}{2} \sinh(\frac{k_u x}{\sqrt{2}}) [\cos(k_u z) e^{\pm \frac{k_u y}{\sqrt{2}}} - \cos(k_u z - k_u (\frac{\lambda_u}{4} + \delta)) e^{\mp \frac{k_u y}{\sqrt{2}}}] \\ \frac{B_0}{2} \cosh(\frac{k_u x}{\sqrt{2}}) [\cos(k_u z) e^{\pm \frac{k_u y}{\sqrt{2}}} + \cos(k_u z - k_u (\frac{\lambda_u}{4} + \delta)) e^{\mp \frac{k_u y}{\sqrt{2}}}] \\ \pm \frac{B_0 \sqrt{2}}{2} \cosh(\frac{k_u x}{\sqrt{2}}) [-\sin(k_u z) e^{\pm \frac{k_u y}{\sqrt{2}}} + \sin(k_u z - k_u (\frac{\lambda_u}{4} + \delta)) e^{\mp \frac{k_u y}{\sqrt{2}}}] \end{bmatrix} \quad (1)$$

The magnetic field of the displaced PCU on axis is

$$\mathbf{B}(z) = B_0 \cos(k_u(z - \Delta)) \left[\cos(k_u \Delta) \hat{j} + (-1)^d \sin(k_u \Delta) \hat{k} \right], \quad (2)$$

* Work supported by Institute for Research in Fundamental Sciences (IPM)

[†] nsmirian@ims.ac.jp

where $\Delta = \lambda/8 + \delta/2$ is the half longitudinal displacement, and d is an even number for b' section and an odd number for $\#$ section.

Following the Colson's analysis [4], we can find the the zero order dimensionless velocities of electrons. For the transverse velocities we obtain:

$$\beta_y(z) = (\beta_0 - (-1)^d \beta_z(z)) \tan(\Delta), \quad (3)$$

$$\beta_x = \beta_0 \left(2(-1)^d \tan^2(\Delta) \left(\frac{\beta_z}{\beta_0} \right) - \left(\frac{\beta_z}{\beta_0} \right)^2 (\tan^2(\Delta) + 1) - (\tan^2(\Delta) - 1) \right)^{1/2} \quad (4)$$

and for longitudinal velocity we find

$$\begin{aligned} & (-1)^d \sin^2(\Delta) \left(\sin^{-1} \left(\frac{\beta_z}{\beta_0} - (-1)^d \tan^2(\Delta) \right) - \frac{\pi}{4} \right) \\ & - \sqrt{\cos^2(\Delta) - \left(\frac{\beta_z}{\beta_0} - (-1)^d \sin^2(\Delta) \right)^2} \\ & = \frac{-eB_0}{k_u \gamma m c^2} \sin(k_u z - \Delta). \quad (5) \end{aligned}$$

Further, simplification of the above Equations is impossible. In case of $\Delta = 0$ in Eq. (5), the simple longitudinal velocity equation in normal planar undulator, $\beta_z/\beta_0 = 1 - (eB_0/2\gamma m c^2 k_u)^2 \sin^2(k_u z)$ can be obtained. Since the resonance condition, and radiation spectrum are obtained from the longitudinal velocity, one expects the resonance and spectrum equation in the PCUs to be different from those in the normal undulator.

In the FEL analysis, by using the electron velocity and the radiation electromagnetic fields, variation of electron energy and radiation field equations can be obtained. Further, the gain lengths of radiation wave can be found by means of the standard linear analysis of the variation of electron energy and radiation field equations. However, working with the velocity equations in the PCUs is not straight forward, we need simpler longitudinal velocity to calculate the resonance equation, FEL gain length, FEL parameters and pendulum equation. In other words, the FEL analysis is not easy in the PCUs. So, in order to extract the radiation wave evolution and information, we prefer to go straight to the simulation [5].

The electromagnetic field in simulation is assumed to be in the form of Gauss-Hermit modes that can be explained in terms of a complete basis set consistent with the planar undulator. The vector potential can be expressed as

$$\mathbf{A}(x, t) = \hat{e}_x \sum_{l,n,h} e_{l,n,h}(x, y) [A_{l,n,h}^{(1)} \cos \varphi_h + A_{l,n,h}^{(2)} \sin \varphi_h] \quad (6)$$

where summations over l and n denote the transverse modes, h is the harmonic number, $A_{l,n,h}^{(1,2)}$ are the slowly varying complex radiation field amplitudes, and

$$e_{l,n,h}(x, y) = \exp(-r^2/w_h^2) H_l(\sqrt{2}x/w_h) H_n(\sqrt{2}y/w_h)$$

represents the transverse structure of each mode, where H_r is the Hermit polynomial and w_h is the waist of the h^{th} harmonic. In this equation, $\varphi_h = h(k_0 z - \omega_0 t) + \alpha_h r^2/w_h^2$ is the vacuum phase while $k_0 (= \omega_0/c)$ is the vacuum wave-number and α_h is the curvature of the phase front. It is assumed that $A_{l,n,h}^{(1,2)}$, α_h , and w_h are slowly varying function of z .

Substituting Eq. (6) into Maxwell's equations and using slowly varying envelope approximation, leads to a parabolic diffusion equation for the harmonic amplitudes, that can be averaged over one wave period to obtain an equation for the vector potential.

The momentum equation of motion for electrons can be obtained by inserting the electric and magnetic fields of radiation as well as the undulator magnetic field in the relativistic Lorentz force equation.

SIMULATION RESULTS

The set of coupled nonlinear differential equations for the undulator magnetic field and radiation electromagnetic field, as well as the electron momentum equations can be solved numerically by the Cyrus 3D code [6]. The simulation was done in time independent approximation. The wiggler parameters in all cases of PCUs are $\lambda_u = 3.3$ cm, $B_0 = 4.8$ kG. Also we choose an entrance taper region of $N_i = 10$ undulator period in length such that the tapered magnetic field amplitude is $B_0 \sin^2(k_0 z/4N_i)$. The electron current I has been fixed at 150 A, with the initial radius $r_b = 0.015$ cm, while the electron energy is chosen as 200 MeV. The thermal and the diffraction effects of the electron beam are ignored.

The initial conditions of the radiation fields is assumed such that the fundamental wavelength is seeded with a 5 W of optical power which is totally in the lowest mode of the fundamental resonance. The initial radiation waist is assumed to be 0.05 cm and the initial alpha parameter is zero.

For the displacement PCU simulation, we choose the longitudinal displacement $\delta = 0.008\lambda_u$ to have an adjustment such that the vertical force becomes 0.5% of the maximum force between the two arrays. By considering Eq. (3) in Ref. [3], the deflection parameter for the PCU with this displacement becomes 1.019. With this condition the resonance wavelength is found approximately to be 156.75 nm. Note that the resonance wave length is found from several simulations.

In Fig. 2, the comparison of the fundamental and the third harmonic radiation power growth for different number of sections in the displaced PCU with $D=400$, $D=100$, $D=10$, and $D=2$ with the normal undulator (NU) with the same undulator deflection ($K=1.019$), are presented as a function of the distance through the undulator. To keep the K value in the normal undulator the magnetic field is chosen as

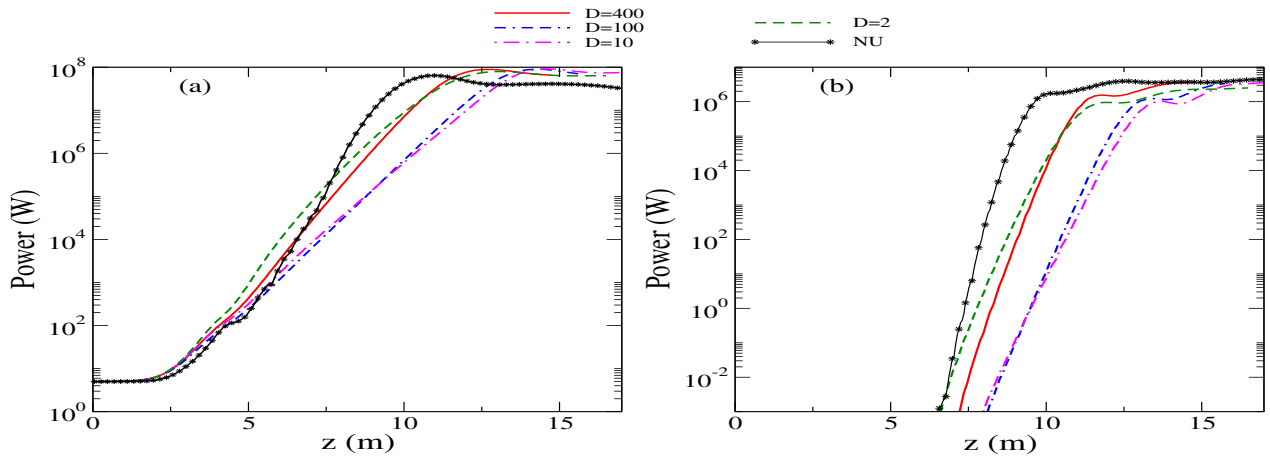


Figure 2: Power growth of (a) the fundamental resonance and (b) the third harmonic in the displaced PCUs with D sections and normal undulator (NU).

Table 1: The optical characteristics of the saturation point of the fundamental resonance and the third harmonic in different displaced PCUs with D sections and in the normal undulator (NU).

	NU	PCU, D=400	PCU, D=100	PCU, D=10	PCU, D=2
α_1	0.44	0.38	0.36	0.28	0.46
α_3	0.99	0.59	0.9	0.5	1.43
w_1	0.26 mm	0.28 mm	0.28 mm	0.25 mm	0.4 mm
w_3	0.14 mm	0.16 mm	0.19 mm	0.16 mm	0.27 mm

$B=3.31$ KG. In the PCU with $D=400$ sections, the length of each section is equal to the period of the undulator λ_u . Obviously the number of sections in the PCU can change the gain length of the radiation power growth. As can be seen from Fig. 2 (a), the radiation in the normal undulator saturates near $z = 11$ m with the power of $P_s = 68$ MW, while in the phase combined undulator with 400 sections, the saturation point is near $z = 12.8$ m and the power is $P_s = 86$ MW. Likewise when the number of sections is $D = 100$, $D = 10$, and $D = 2$ the saturation point, respectively, are located at $z = 14.5$, 14.8 , and 13.5 m; while the saturation powers are, respectively, $P_s = 64$, 64 , and 57 MW. The average gain length of radiation in the normal undulator is $L_g = 55$ cm and in the PCU with different sections of $D = 400$, 100 , 10 , and 2 is, respectively, $L_g = 66$, 77 , 79 , and 71 cm.

In Fig. 2 (b) where the third harmonic power growth curves are compared, we can observe that the third harmonic power reaches saturation at ($z_s = 10$ m, $P_s = 1.7$ MW) in normal undulator and in 400, 100, 10, 2-section PCU reaches saturation, respectively, at ($z_s = 11.5$ m, $P_s = 1.3$ MW), ($z_s = 13.5$ m, $P_s = 0.81$ MW), ($z_s = 13.8$ m, $P_s = 0.62$ MW), and ($z_s = 12$ m, $P_s = 0.44$ MW). From these figures it can be seen that the gain length and the saturation point of the normal undulator are shorter than that of the PCUs, and the saturation power in normal undulator and 400-section PCU is higher than that in the PCUs. In the following, we consider the properties of radiation of the fundamental and third harmonic at saturation points for these undulators.

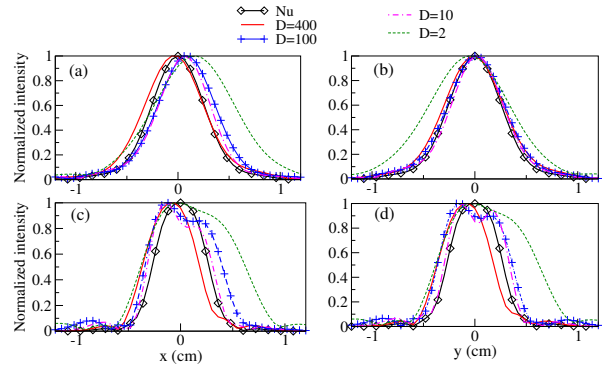


Figure 3: Normalized intensity in the x and y direction for (a) the fundamental resonance (b) the 3rd harmonic radiation in different displaced D-section PCUs and normal undulator (NU).

Table 1 reports the phase front curvature and the waist of the fundamental resonance (α_1 and w_1), and the third harmonic (α_3 and w_3) at the saturation point of each undulator. The phase front curvature of radiation at the saturation point in 2-section PCU and normal undulator is higher than that in other PCUs. Also the radiation waist in the PCU with two sections is wider than that in other PCUs and the normal undulator.

Figures 3(a) and (c) illustrate the fundamental resonance and third harmonic normalized intensity distribution, respec-

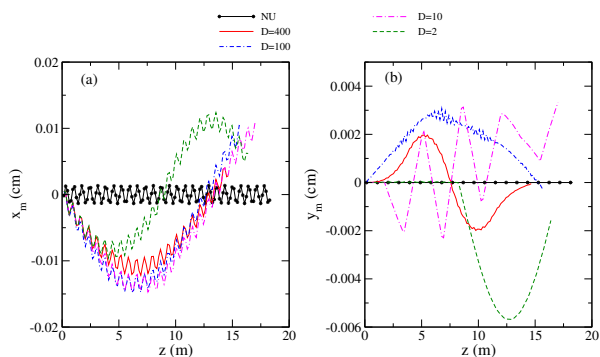


Figure 4: The center of mass motion of the bunch through the undulator in (a) x and (b) y directions for different cases.

tively, in the x direction; and Figures 3(b) and (d) show those in y direction for different D values. It is clear that the standard deviation of the normalized intensity radiation in the case of normal undulator is less than other cases. And the standard deviation of radiation in two-section PCU is wider than other cases. Further, Fig. 3(d) shows the y-distribution of the third harmonic radiation in the cases of PCU with 100 and 10 sections have two peaks near $y = -0.13$ cm and $y = 0.9$ cm.

Actually, at the beginning and end of each PCU section (b and # section), magnetic field changes, which modifies the transverse dynamics of electrons. Mathematically, the transverse coordinate y of the electrons are continuous but its first and second derivatives, that correspond to the momentum and acceleration, respectively, are not continuous. This means that we have critical points in electron dynamics at the beginning of each section of PCU. Figure 4 presents the center of mass motion of the bunch through the undulator in the x and y directions for different cases. In normal undulator, the center of mass motion of the bunch in the x and y directions oscillates very rapidly around the ori-

gin. There is a large kick in the y-trajectory of electron in the middle of the undulator, which is due to the switch from section b to section #. In section b the velocity of the electron in the y direction is $\beta_y(z) = (\beta_0 - \beta_z(z))1.05$, but in section # the electron velocity in the y direction is $\beta_y(z) = (\beta_0 + \beta_z(z))1.05$.

SUMMARY

This report focuses on studying simulation of FEL amplifier with a displaced phase-combined undulator, in which a magnetic attractive force is eliminated. By obtaining the electron velocity components on the axis of the displaced PCU, we have shown that analysis of the FEL and finding important FEL parameters by employing the linear analysis in the PCUs is not straight forward. Also, calculation of resonance condition with longitudinal velocity of the electrons in PCUs is not straight forward. Then the simulation of radiation and electron motion has been performed. The radiation properties of the fundamental resonance and the third harmonic through the displaced PCUs and normal undulator with the same undulator deflection parameter are compared. Some differences in saturation length and saturation power were found.

REFERENCES

- [1] W. Ackermann, G. Asova, V. Ayvazyan, A. Azima, and N. Baboi, Nat. Photon. 1, 336 (2007).
- [2] B. McNeil, Nat. Photonics 3, 375 (2009).
- [3] R. Kinjo, T. Tanaka, Phys. Rev. ST Accel. Beams 17, 122401 (2014).
- [4] W.B. Colson, IEEE Journal of Quantum Electronics QE-17, 1417 (1981).
- [5] N.S. Mirian, E. Salehi, et al., submitted to publication (2015).
- [6] M. H. Rouhani, N. S. Mirian, S. Salehi, reference available at, <http://particles.ipm.ir/Cyrus1D.jsp>